

## Supporting Information

# Mesoporous Ni-Fe oxide multi-composite hollow nanocages for efficient electrocatalytic water oxidation reactions

Bong Kyun Kang,<sup>‡a</sup> Moo Hyun Woo,<sup>‡a</sup> Jooyoung Lee,<sup>a</sup> Young Hyun Song,<sup>a</sup> Zhongli Wang,<sup>b</sup>  
Yanna Guo,<sup>b</sup> Yusuke Yamauchi,<sup>b,c</sup> Jung Ho Kim,<sup>b,c</sup> Byungkwon Lim<sup>a</sup> and Dae Ho Yoon<sup>a\*</sup>

<sup>a</sup>School of Advanced Materials Science and Engineering, Sungkyunkwan University (SKKU),  
Suwon 440-746, Republic of Korea,

<sup>b</sup>International Research Center for Materials Nanoarchitectonics (MANA), National Institute for  
Materials Science (NIMS), 1-1 Namiki, Tsukuba, Ibaraki 305-0044, Japan,

<sup>c</sup>Australian Institute for Innovative Materials (AIIM), University of Wollongong, Squires Way,  
North Wollongong, NSW 2500, Australia,

Corresponding to E-mail : [dhyoon@skku.edu](mailto:dhyoon@skku.edu) (D. H. Yoon)

<sup>‡</sup> B. K. Kang and M. H. Woo contributed equally to this work.

## Experimental

### **Synthesis of $\text{Ni}_3[\text{Fe}(\text{CN})_6]_2$ prussian blue analogue (PBA) nanocube precursors and mesoporous $\text{NiO}/\text{NiFe}_2\text{O}_4$ multi-composite hollow nanocages (NCs).**

We synthesized uniform  $\text{Ni}_3[\text{Fe}(\text{CN})_6]_2$  PBA nanocube precursors by modifying an established procedure.<sup>1</sup> In a typical synthesis, we dissolved 0.1374 mmol of Nickel (II) acetate tetrahydrate (97 %,  $\text{Ni}(\text{CH}_3\text{COO})_2 \cdot 4\text{H}_2\text{O}$ , DAEJUNG, Korea), 0.7174 mmol of Sodium dodecylbenzenesulfonate (SDBS) (technical grade (Aldrich),  $\text{C}_{18}\text{H}_{29}\text{NaO}_3\text{S}$ , Sigma-Aldrich, USA) in 25 ml of D. I. water to form solution A. We dissolved 0.1502 mmol of Potassium hexacyanoferrate (III) (ACS reagent,  $\geq 99.0$  %,  $\text{K}_3[\text{Fe}(\text{CN})_6]$ , Sigma-Aldrich, USA) in 25 ml of D. I. water to form solution B. Solutions A and B were heated at 60 °C oil bath with stirring for 1 h, respectively. Then solutions A and B were mixed and stirred in 60 °C oil bath for 3 h. After collection by centrifugation and washing with ethanol several times, the precipitates were dried in 60 °C oven overnight. Using the hydrothermal method, the prepared monodispersed  $\text{Ni}_3[\text{Fe}(\text{CN})_6]_2$  PBA nanocube precursors were calcined in air at 500 ~ 700 °C with a heating rate of 5 °C  $\text{min}^{-1}$  for 1 hour to transform them into mesoporous  $\text{NiO}/\text{NiFe}_2\text{O}_4$  multi-composite hollow NCs. In addition, pure  $\text{NiFe}_2\text{O}_4$  and  $\text{NiO}/\text{NiFe}_2\text{O}_4$  nanoparticles were prepared at 500 °C for 5 h in Air atmosphere by using liquid phase precursor method.<sup>2</sup>

### **Materials characterization.**

We observed the surface morphology of the  $\text{Ni}_3[\text{Fe}(\text{CN})_6]_2$  PBA nanocube precursors and mesoporous  $\text{NiO}/\text{NiFe}_2\text{O}_4$  multi-composite hollow CNs by field-emission scanning electron microscopy (FESEM, JEOL 7500F). We carried out high-resolution transmission electron

microscopy and energy dispersive spectroscopy (EDS) mapping using a JEM2100F with an accelerating voltage of 200 kV. The crystallinity and structure of the  $\text{Ni}_3[\text{Fe}(\text{CN})_6]_2$  PBA nanocube precursors and mesoporous  $\text{NiO}/\text{NiFe}_2\text{O}_4$  multi-composite hollow CNs were examined by powder X-ray diffraction (Bruker D8 FOCUS) using  $\text{CuK}\alpha$  radiation. X-ray photoelectron spectroscopy (XPS) and Fourier transform infrared (FTIR, Bruker IFS-66/S) spectroscopy were employed to analyze the chemical bonding within the materials. Thermogravimetry and differential thermal analysis (TG-DTA, Seiko Exstar) was performed in air at a heating rate of  $5\text{ }^\circ\text{C min}^{-1}$  from 30 to  $1000\text{ }^\circ\text{C}$ , to confirm the reaction of  $\text{Ni}_3[\text{Fe}(\text{CN})_6]_2$  PBA nanocubes and the crystallization of  $\text{NiO}/\text{NiFe}_2\text{O}_4$  multi-composite. We measured the Brunauer–Emmett–Teller specific surface areas and the Barrett–Joyner–Halenda pore size distributions of the samples on the surface area by using a pore size analyzer (Autosorb-iQ 2ST/MP) at 77 K with  $\text{N}_2$  gas.

### **Electrochemical measurements.**

All electrochemical experiments were conducted on a CHI 660D (ALS, Japan) electrochemistry workstation using a three-electrode cell. SCE (Saturated Calomel Electrode) was used as the reference electrode, and graphite rod was used as the counter electrode. The working electrode was prepared by mixing  $\text{NiO}/\text{NiFe}_2\text{O}_4$  powder, carbon black (Vulcan XC 72R) as a conductive agent, and nafion as a binder (8:1:1 in weight ratio) in 1 mL of 2:1 v/v water/isopropanol mixed solvent. After sonication for 30 min, the slurry was coated onto carbon paper ( $1\text{ cm} \times 1\text{ cm}$ , Toray, Japan), and dried at room temperature. The catalyst loading for  $\text{NiO}/\text{NiFe}_2\text{O}_4$  was about  $1\text{ mg cm}^{-2}$ . The polarization curves were obtained in 1 M KOH with a scan rate of  $5\text{ mV s}^{-1}$  at room temperature. All potentials were iR-compensated and converted to a reversible hydrogen electrode

(RHE) scale via calibration. And the presented current density was normalized to the geometric surface area.

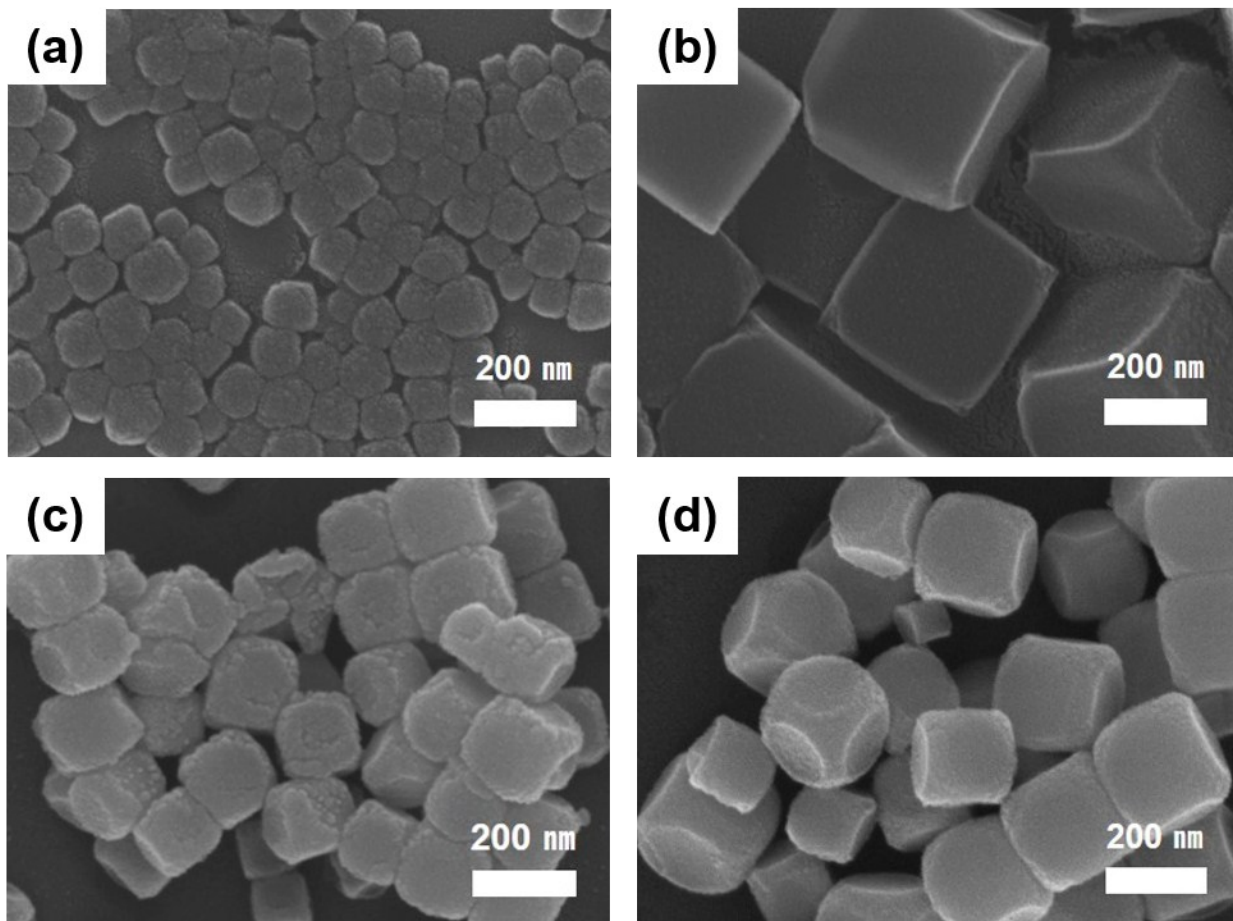


**Fig. S1.** FESEM images of synthesized  $\text{Ni}_3[\text{Fe}(\text{CN})_6]_2$  PBA nanocubes; concentration of SDBS (a) 0.3587 and (b) 1.4348 mmol at 60 °C, temperature (c) 50 and (d) 70 °C with concentration of SDBS 0.7174 mmol.

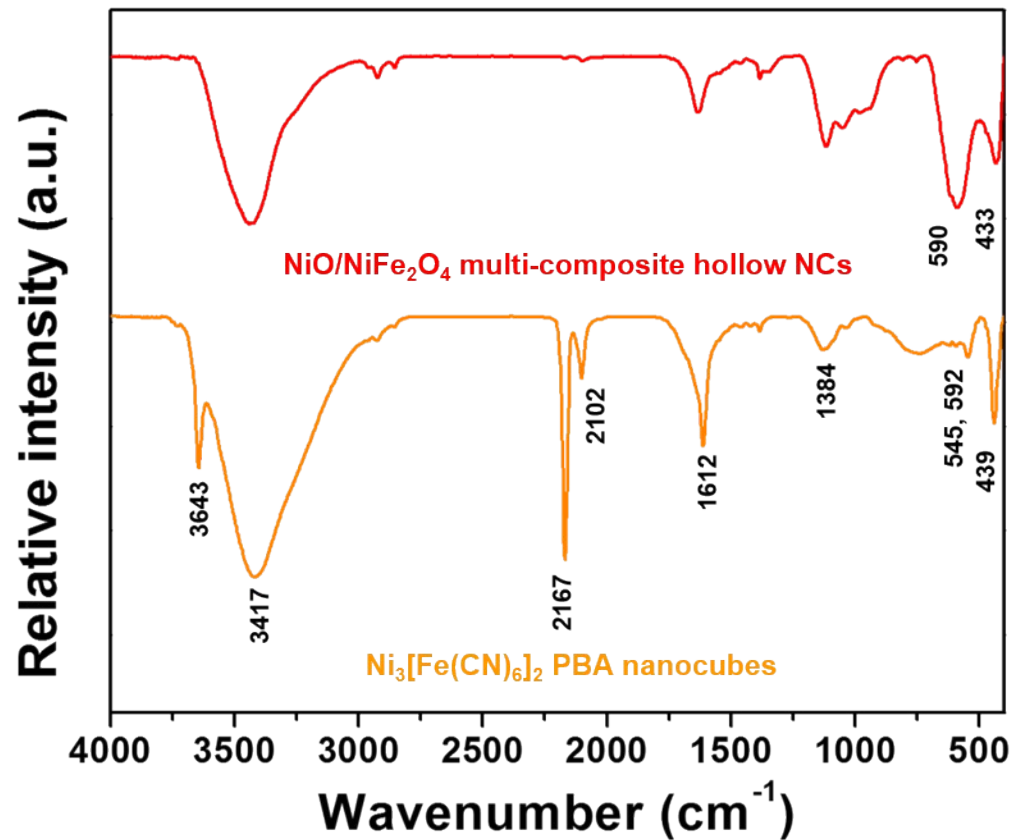


**Fig. S2.** FTIR spectra of the as-prepared Ni<sub>3</sub>[Fe(CN)<sub>6</sub>]<sub>2</sub> PBA nanocubes and mesoporous NiO/NiFe<sub>2</sub>O<sub>4</sub> multi-composite hollow NCs.

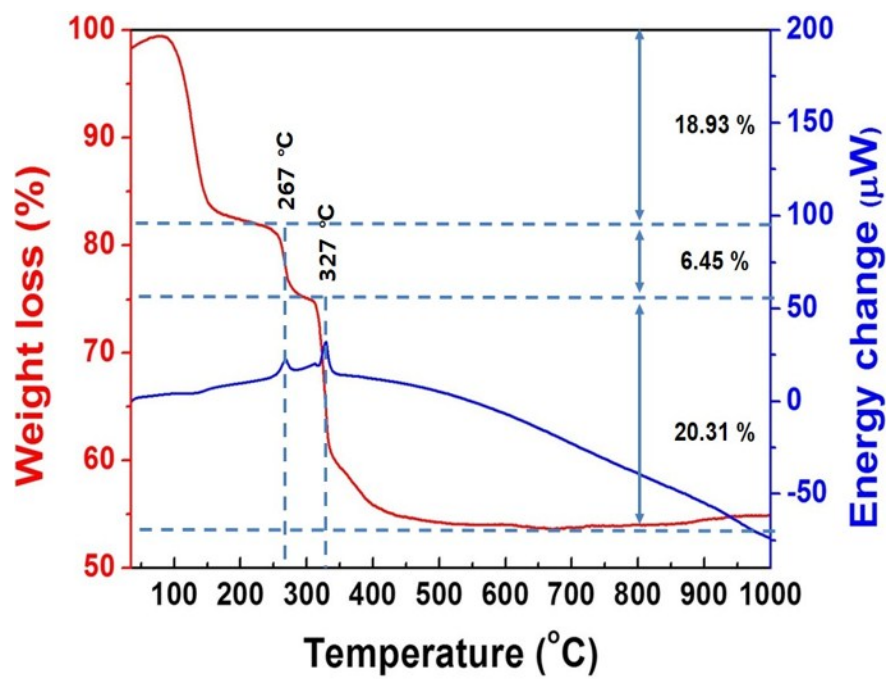


**Fig. S3.** TG-DTA curves of  $\text{Ni}_3[\text{Fe}(\text{CN})_6]_2$  PBA nanocubes.

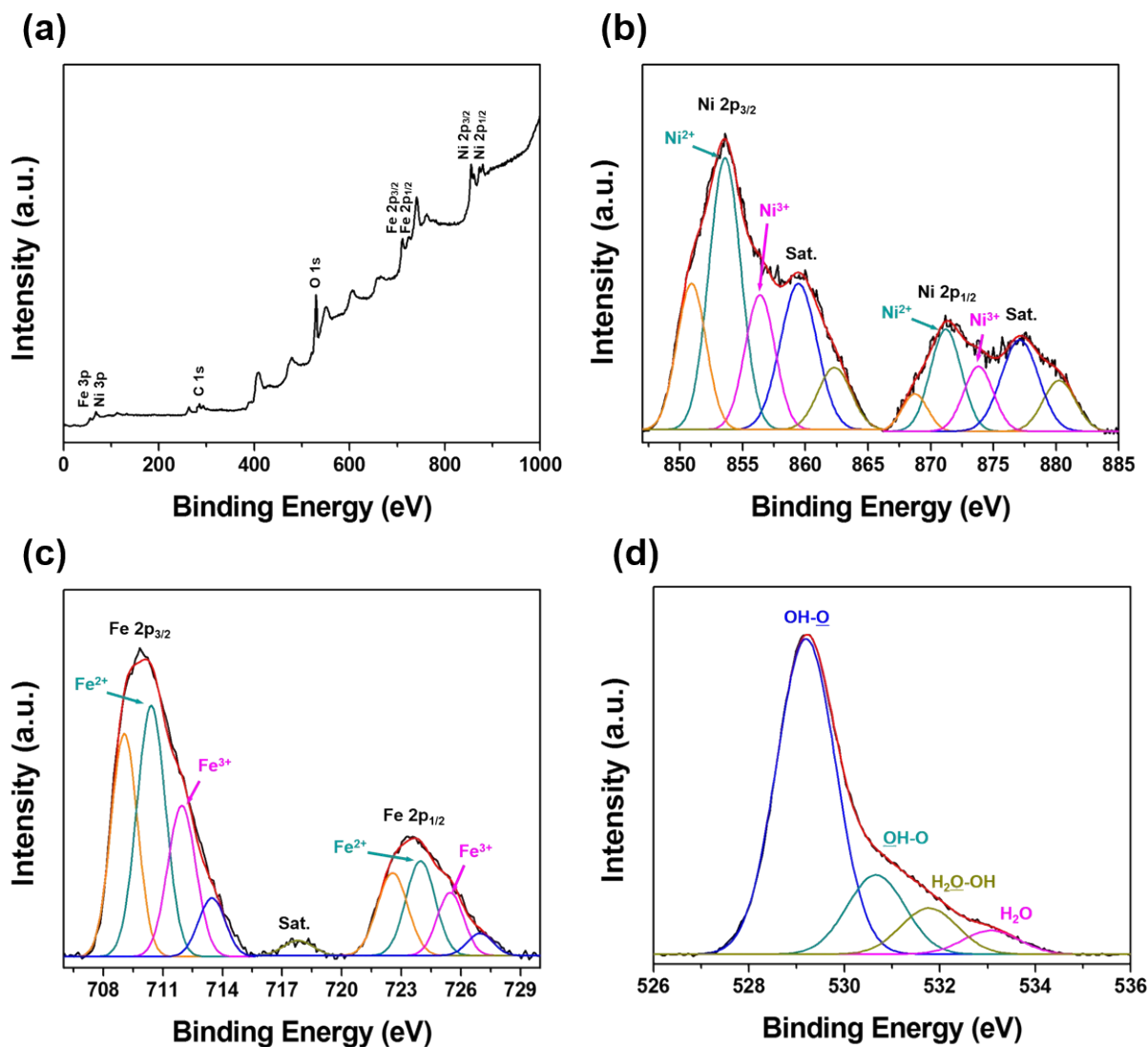


**Fig. S4.** (a) XPS survey scan of NiO/NiFe<sub>2</sub>O<sub>4</sub> multi-composite hollow NCs after 1 h of calcination in air at 500 °C. XPS spectra of (b) Ni 2p, (c) Fe 2p, and (d) O 1s of NiO/NiFe<sub>2</sub>O<sub>4</sub> multi-composite hollow NCs sample.



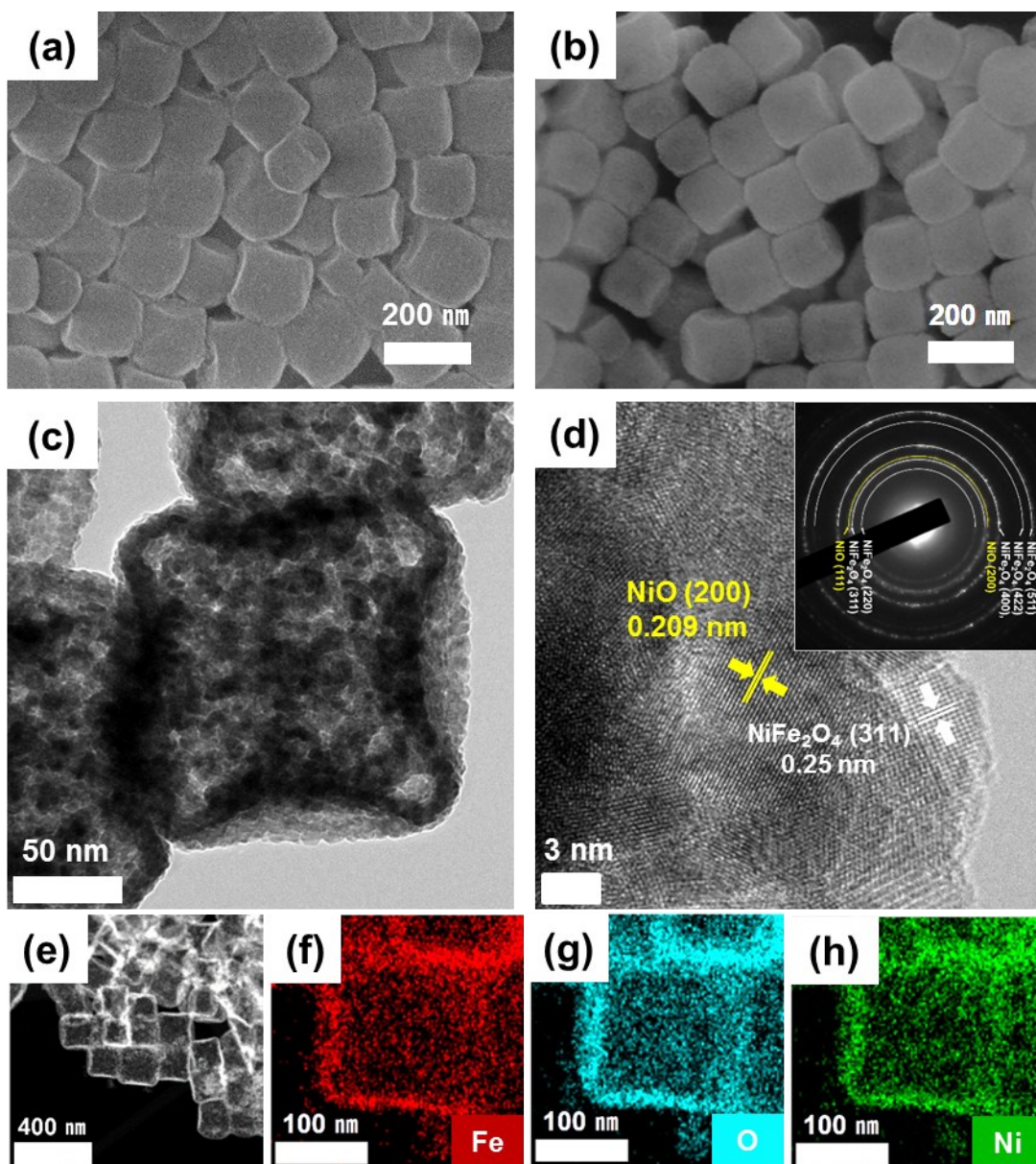


**Fig. S5.** (a) and (b) FESEM images of NiO/NiFe<sub>2</sub>O<sub>4</sub> multi-composite hollow NCs after 1 h of calcination in air at 600 and 700 °C. (c) TEM and (d) HRTEM images (the inset shows the corresponding selective area diffraction pattern) of mesoporous NiO/NiFe<sub>2</sub>O<sub>4</sub> multi-composite hollow NCs after 1 h of calcination in air at 600 °C. (e)-(h) STEM-EDS of mesoporous NiO/NiFe<sub>2</sub>O<sub>4</sub> multi-composite hollow NCs.

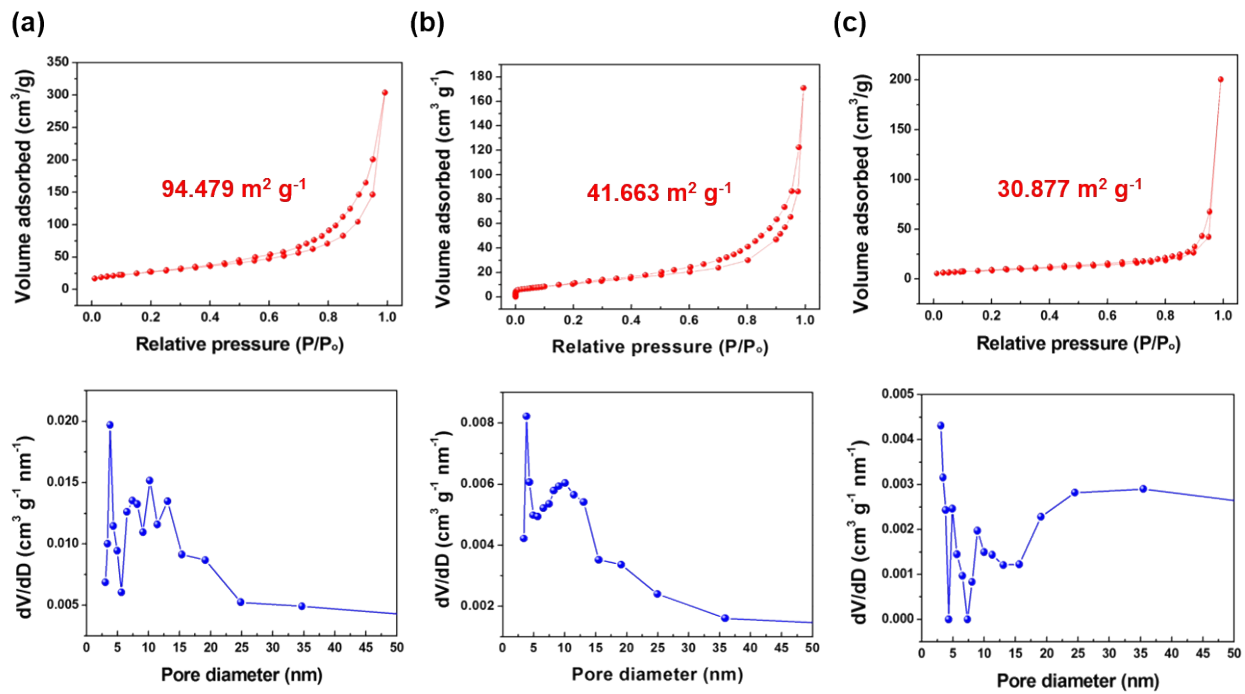


**Fig. S6.** Nitrogen adsorption-desorption isotherms and pore size distribution of mesoporous NiO/NiFe<sub>2</sub>O<sub>4</sub> multi-composite hollow NCs; (a) 500 °C, (b) 600 °C, and (c) 700 °C for 1 hour at air atmosphere.

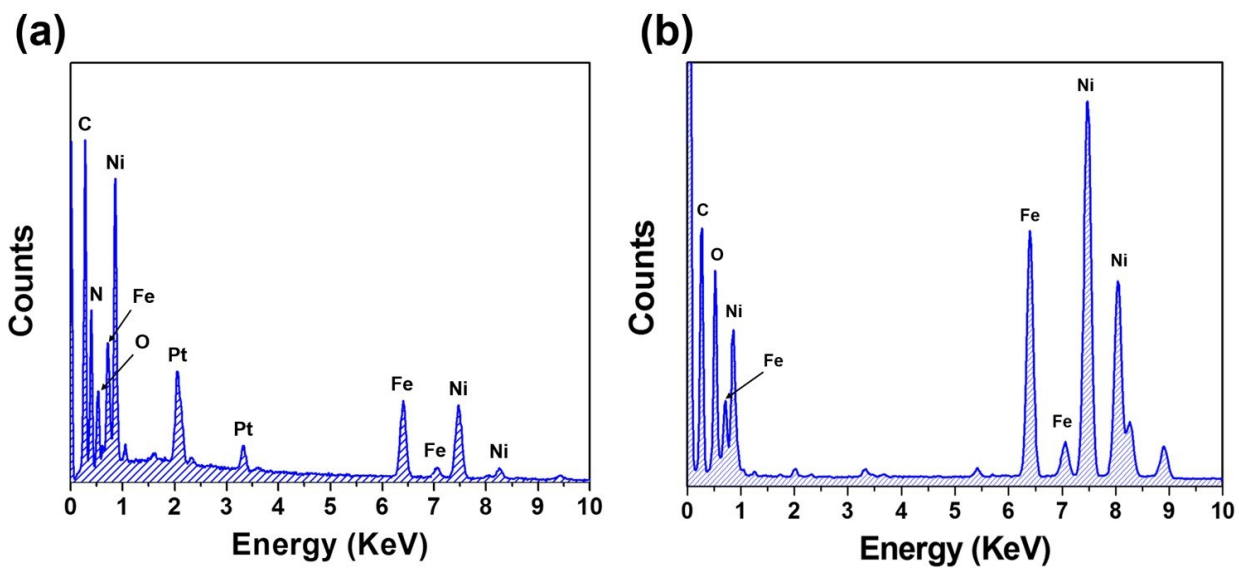


**Fig. S7.** The EDS spectra of the as-prepared (a)  $\text{Ni}_3[\text{Fe}(\text{CN})_6]_2$  PBA nanocubes and (b) mesoporous  $\text{NiO}/\text{NiFe}_2\text{O}_4$  multi-composite hollow NCs after calcined at  $500\text{ }^\circ\text{C}$  for 1 hour.

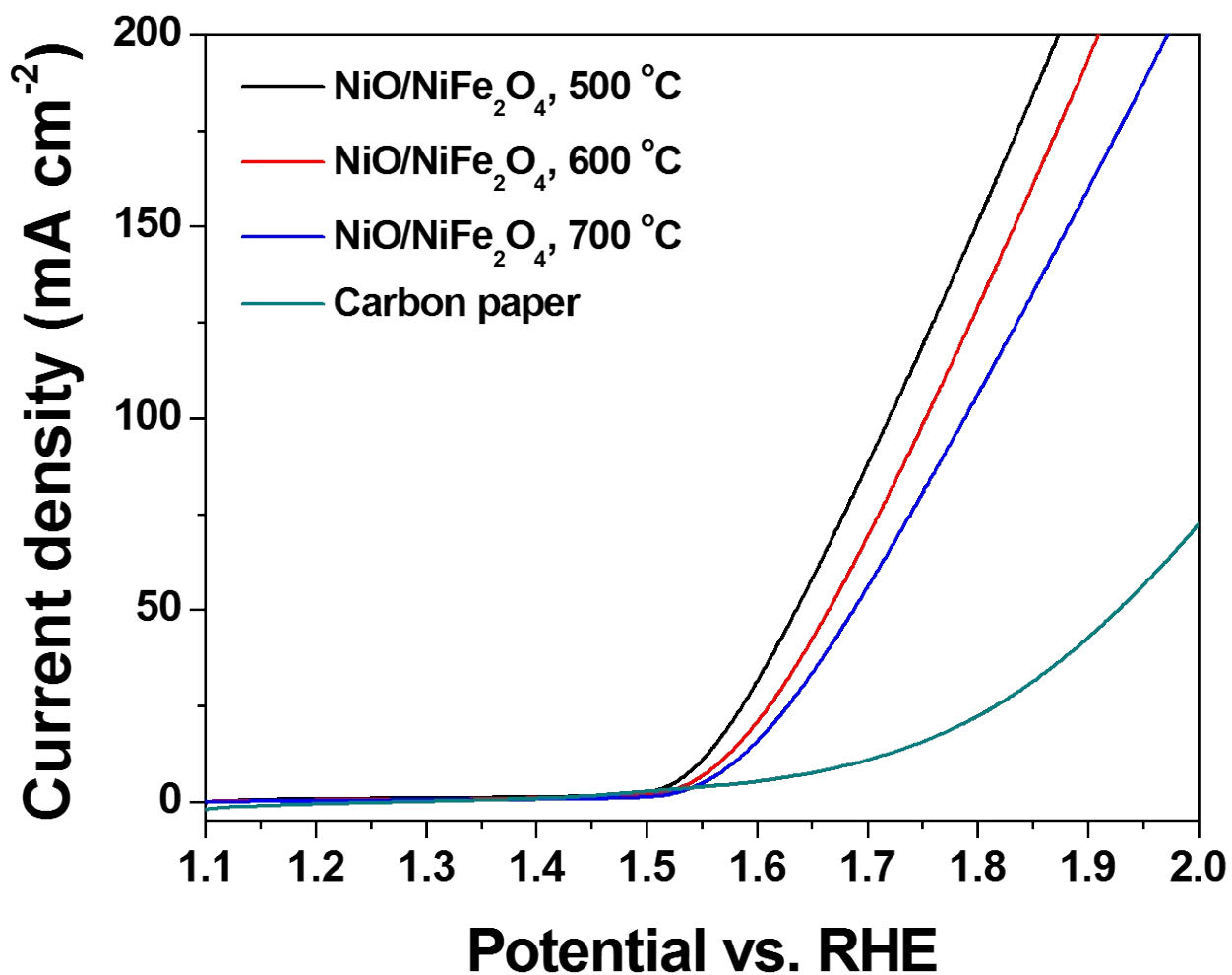


**Fig. S8.** Comparison of electrocatalytic properties of NiO/NiFe<sub>2</sub>O<sub>4</sub> multi-composite hollow NCs (500, 600, and 700 °C), and pristine substrate. OER polarization curves recorded in 1 M KOH solution at a scan rate of 5 mV s<sup>-1</sup> without iR compensation.

**Table S1.** Comparison of electrocatalytic properties of NiO/NiFe<sub>2</sub>O<sub>4</sub> multi-composite hollow NCs (500, 600, and 700 °C), pure NiFe<sub>2</sub>O<sub>4</sub>, NiO and mixed NiO/NiFe<sub>2</sub>O<sub>4</sub>.

| <b>Sample</b>  | <b>Overpotential (mV)<br/>at 10 mA cm<sup>-2</sup></b> | <b>Tafel polt (mV dec<sup>-1</sup>)</b> |
|--|--|---|
| <b>NiO/NiFe<sub>2</sub>O<sub>4</sub> multi-composite hollow NCs (500 °C)</b> | 303  | 58.5                                    |
| <b>NiO/NiFe<sub>2</sub>O<sub>4</sub> multi-composite hollow NCs (600 °C)</b> | 322  | 64.9                                    |
| <b>NiO/NiFe<sub>2</sub>O<sub>4</sub> multi-composite hollow NCs (700 °C)</b> | 335  | 67.8                                    |
| <b>NiFe<sub>2</sub>O<sub>4</sub></b>   | 323  | 54                                      |
| <b>NiO/NiFe<sub>2</sub>O<sub>4</sub></b>                                     | 327  | 73                                      |
| <b>NiO (commercial)</b>  | 423  | 96                                      |
| <b>NiO (commercial)/NiFe<sub>2</sub>O<sub>4</sub></b>                        | 334  | 89                                      |

## Supporting References

1. P. Nie, L. Shen, H. Luo, B. Ding, G. Xu, J. Wang and X. Zhang, *J. Mater. Chem. A.*, 2014, **2**, 5852.
2. B. K. Kang, M.-O. Kim, D. H. Yoon, *Mater. Lett.*, 2012, **79**, 170.